

Measurements of IR Spectra and Thermophysical Properties of Tetragonal Zirconia by Thermal Radiation Calorimetry

Hirokazu TANAKA, Shinya SAWAI, Kohsuke MORIMOTO and Kumao HISANO

Department of Applied Physics, National Defense Academy, Yokosuka 239-8686, Japan

(Received May 12, 2000; accepted for publication July 24, 2000)

Normal emission spectra from a clear surface of tetragonal zirconia ceramic stabilized by 5.3 wt% yttria are measured in the frequency range of 200–4500 cm^{-1} . The values of the hemispherical total emissivity are derived from a spectral analysis based on virtual mode equations and Kramers-Krönig relations. With these values, thermal conductivity data are obtained from measurements of temperature gradients in the sample at temperatures between 400 K and 850 K. Heat capacity measurements are carried out by quasi-static thermal radiation calorimetry. The present results are consistent with data in the literature obtained by other methods. Based on the comparison of the spectral reflectivity with the emission spectrum, it is suggested that the effects of radiation heat transfer in the ceramic sample may be compensated for by the scattering process of grain boundaries.

KEYWORDS: hemispherical total emissivity, thermal radiation, emission spectrum, thermal conductivity, specific heat capacity, tetragonal zirconia, yttria-stabilized

1. Introduction

Thermal radiation calorimetry (TRAC) has been developed for simultaneous measurements of thermophysical and dielectric properties, in which the radiation heat transfer between a disk-shaped sample and a heater in a vacuum chamber has been considered under several geometrical conditions.^{1–4)} For the specific heat capacity measurement, the sample was heated on both surfaces. Thermal conductivity was determined from measurements of the temperature gradient in the sample and the radiant power from the sample heated on the back surface. **In these calorimeters, both disk surfaces of the sample were blackened with a material whose surface emissivity is known and calibration processes with a reference material were required.**

Recently, we proposed a method to derive the hemispherical total emissivity from the normal emission spectrum of the bare surface of a sample.⁵⁾ The basic idea refers to virtual mode equations for an ionic crystal slab,⁶⁾ in which the spectral response of the slab is given as a function of emission angle, slab thickness and the dielectric response function. It is well known that the dielectric function can be derived from a Kramers-Krönig analysis of the normal spectral reflectivity. For this analysis, we derived the normal reflection spectrum from the normal emission spectrum on the basis of Kirchhoff's law for thermal radiation. Consequently, we obtained the hemispherical total emissivity and the thermal conductivity of silicate glasses by TRAC without blackening. The samples suitable for testing this method are thermally insulating materials in which transmission may occur at higher frequencies in the IR region, because the radiation heat transfer caused by transmission in the sample may become an error source in the values of thermal conductivity through the emissivity. The effects of radiation scattering in the sample were neglected in the previous study.⁵⁾

In ceramics such as zirconia in which transmission occurs at lower frequencies than in silicate glasses, the effects of transmission as well as radiation scattering in the sample may become large. However, the scattering process by grain boundaries in a ceramic sample is expected to decrease the effects of the radiation heat transfer on the values of thermal conductivity. Zirconia ceramics are remarkable materi-

als because of their excellent mechanical and electrochemical properties at high temperature. It is known that the high-temperature tetragonal and cubic phases^{7,8)} of zirconia are stabilized at room temperature by doping different contents of yttria,⁹⁾ although the room-temperature phase of pure zirconia takes a monoclinic structure.¹⁰⁾ Among these phases, a tetragonal zirconia stabilized by 5.3 wt% yttria is considered to be one of the standard materials for thermal insulation coating.^{11,12)}

In this paper, the spectral TRAC mentioned above is applied to the tetragonal zirconia of a fine ceramic. The hemispherical total emissivity of the tetragonal zirconia is derived from the normal emission spectra between 400 K and 850 K. With this emissivity, the thermal conductivity is obtained by TRAC at steady state. The specific heat has been measured from 540 K to 840 K by quasi-static TRAC. The present results for the thermal conductivity and the specific heat capacity are compared with those obtained by different techniques.^{11,13)} The effects of radiation heat transfer and scattering in the sample are also investigated.

2. Theoretical background

2.1 Thermal conductivity

TRAC theory has been described in detail in the previous paper.²⁾ Let us suppose that a disk shaped sample with thickness d is heated on one face (S_1) by a flat heater in a vacuum chamber. Another surface (S_0) of the sample is not blackened in the present setup for spectral emissivity measurement. If we assume that the temperature distribution in the sample is one dimensional and linear, we can express the conductive heat flow from surface S_1 at temperature T_1 to S_0 at T_0 as $\lambda(T_1 - T_0)/d$, using the thermal conductivity λ . On the other hand, the radiant power from the surface S_0 to the chamber at temperature T_r is given by $\varepsilon\sigma(T_0^4 - T_r^4)$ with the hemispherical total emissivity ε of S_0 and the Stefan-Boltzmann constant σ . These two expressions of the heat flow should satisfy Kirchhoff's law at boundary S_0 , that is,

$$\lambda(T_1 - T_0)/d = \varepsilon\sigma(T_0^4 - T_r^4). \quad (1)$$

The effects of radiation heat transfer, including scattering in the sample, are not considered in eq. (1) but are discussed in §4. To obtain λ from the surface temperatures in eq. (1),

we must simultaneously determine ε of the bare surface S_0 , which is usually calculated from the directional emissivity. If we write the latter as $\varepsilon(\nu, \theta)$, where ν and θ are, respectively, the frequency and the emission angle, the hemispherical spectral emissivity, ε_ν , can be calculated by

$$\varepsilon_\nu = 2 \int_0^{\pi/2} \varepsilon(\nu, \theta) \sin \theta \cos \theta d\theta. \quad (2)$$

This gives the hemispherical total emissivity as

$$\varepsilon = \frac{\int_0^\infty \varepsilon_\nu W(\nu, T) d\nu}{\int_0^\infty W(\nu, T) d\nu}, \quad (3)$$

where $W(\nu, T)$ is Planck's emissive power at $T = T_0$. Fuchs *et al.*⁶⁾ have shown that the optical properties of an ionic slab are explicitly described in terms of virtual mode equations if the dielectric function $\xi(\nu)$ is known. In the present case, the directional emission spectrum of an ionic crystal slab on a conducting substrate can be written as

$$\varepsilon(\nu, \theta) = 1 - \frac{1}{2} \left\{ \left| \frac{2 - L_p}{L_p} \right|^2 + \left| \frac{2 - L_s}{L_s} \right|^2 \right\}, \quad (4)$$

where

$$L_p = 1 - i \frac{\beta}{\beta_0 \xi(\nu)} \tan(\beta d), \quad (5)$$

$$L_s = 1 + i \frac{\beta}{\beta_0} \cot(\beta d), \quad (6)$$

with $\beta = 2\pi\nu \{\xi(\nu) - \sin^2 \theta\}^{1/2}$ and $\beta_0 = 2\pi\nu \cos \theta$. On the other hand, the dielectric function is related to the complex refractive index $n_c(\nu)$ as

$$\sqrt{\xi(\nu)} = n_c(\nu) = n(\nu) + ik(\nu), \quad (7)$$

where $n(\nu)$ and $k(\nu)$ are, respectively, the real and imaginary parts of the complex refractive index. Thus, we can calculate the emissivity from the virtual mode equations, knowing the dispersion of the complex refractive index. Prior to the Kramers-Krönig analysis, we refer to the normal emission spectrum $\varepsilon(\nu, 0)$, since it can be transferred to the normal reflection spectrum $R(\nu, 0)$ based on Kirchhoff's law for thermal radiation.^{14,15)} For the frequency range where the sample shows no transmission, it becomes

$$R(\nu, 0) = 1 - \varepsilon(\nu, 0). \quad (8)$$

In the high-frequency range where transmission is observed, Kirchhoff's law can be written as

$$T^*(\nu) + R^*(\nu) + \varepsilon(\nu, 0) = 1, \quad (9)$$

where $T^*(\nu)$ and $R^*(\nu)$ are the apparent transmittance and reflectivity, respectively. If we can estimate the dispersion relation of the refractive index in this region, we are able to calculate $R^*(\nu)$, since the normal reflectivity for unpolarized light is generally given by

$$R^*(\nu) = \left| \frac{n_c(\nu) - 1}{n_c(\nu) + 1} \right|^2. \quad (10)$$

For an ionic crystal slab, transmission usually occurs above the highest longitudinal optical (LO) mode frequency ν_L in the slab. It is well known that the reflectivity becomes zero

at a frequency ν_R slightly above ν_L as long as the sample is a bulk material. On the other hand, $n_c(\nu)$ at very high frequency can be approximated to the refractive index for visible light n_∞ . Consequently, eq. (10) for $\nu \geq \nu_R$ is considered a smooth function with a minimum close to zero around ν_R and asymptotically approaches a constant value given by n_∞ at high frequency. The functional form of the reflectance in this high-frequency region can be estimated from an empirical form of the dielectric function. For simplicity, we shall use a dielectric function with a harmonic oscillator form

$$\xi(\nu) = n_\infty^2 (\nu_L^2 - \nu^2) / (\nu_T^2 - \nu^2), \quad (11)$$

where ν_T is the frequency of the transverse optic (TO) mode responsible for the highest LO mode.

Using eq. (8) for $\nu \leq \nu_R$ and eqs. (9)–(11) for $\nu \geq \nu_R$, we can obtain the complex refractive index through the Kramers-Krönig analysis. It is, however, not preferable to use the imaginary part obtained from eq. (11) for further analysis above ν_R , since eq. (11) is real. On the other hand, the energy of the IR radiation traveling along the optical path length L in a medium with low reflectivity can be written by the absorption coefficient $\alpha(\nu) = 4\pi\nu \cdot k(\nu)$ as

$$T^*(\nu) = e^{-\alpha(\nu)L}. \quad (12)$$

From eqs. (9) and (12) we can estimate $k(\nu)$ for $\nu \geq \nu_R$ where the sample may be transparent for infrared radiation. It is important to note that L must be read as $2d$ for an ionic slab on a perfect metal, because the conducting substrate functions as a perfect mirror.

2.2 Quasi-static TRAC for heat capacity measurement

In order to obtain the specific heat capacity C_p , we must heat the sample in such a way that the temperature distribution in the sample is as small as possible. One of the best ways to do this is to surround the sample with a heater. Let us suppose that one more flat heater is mounted above the sample. When the sample is heated slowly on both sides by the IR radiation, the time rate (dT_s/dt) of the sample temperature (T_s) can be written as¹⁾

$$MC_p \frac{dT_s}{dt} = E_h A_s (I_h - I_s) - E_s A_s (I_s - I_r) - \frac{d}{dt} Q(T_s), \quad (13)$$

where M is the mass, and A_s the surface area of the sample. E_h and E_s are, respectively, the effective emissivities which express heat-exchange coefficients by radiation between the heater and the sample, and between the sample and the environment (vacuum chamber). These coefficients are functions of the surface emissivities of the sample and the heater, and depend on their geometrical configuration in the chamber. The radiant power I_j of the surface covered with a perfect absorber at temperature T_j is given by σT_j^4 , where subscripts $j = s, h$ and r refer to the sample, the heater and the vacuum chamber, respectively. The last term on the right-hand side of eq. (13) is the heat loss per unit time through the thermocouple leads and ceramic pipes supporting the sample. Since we cannot measure the emission spectrum of the sample with the setup for the heat capacity measurement, all surfaces of the sample and the reference disk have to be blackened with the same high emissivity material. Comparing the heating process with the cooling process at the same sample temperature, we obtain^{1,2)}

$$C_p = \frac{E_h A_s (I_h - I'_h) / M}{dT_s/dt - (dT_s/dt)',} \quad (14)$$

where the prime expresses the cooling process. This equation implies that the heat capacity is evaluated with only the one parameter E_h , since the other physical quantities on the right-hand side are directly measurable. The value of E_h for a particular geometrical configuration is easily obtained using a reference sample, whose heat capacity is known, with the same dimensions and blackened surfaces as the sample.

3. Experimental

3.1 Emissivity and thermal conductivity by spectral TRAC at steady state

The sample examined is 5.3(±0.1) wt% yttria-stabilized tetragonal zirconia of a fine ceramic with average grain size of 0.56 μm provided by the Japan Fine Ceramics Center. The density of the present sample is 6.07 g/cm³. The schematic configuration of TRAC for a spectral measurement is illustrated in Fig. 1. This system is enclosed inside a watercooled vacuum chamber. A disk-shaped sample with thickness 5 mm and diameter 24 mm was examined. All surfaces of the sample were polished to optical grade before metal coating. The bottom (S_1) and side surfaces of the sample were coated with copper by vacuum evaporation. The thickness of the copper coat was about 0.1 μm, which was stable for several heating cycles between room temperature and 850 K. Such a metal coating was performed to prevent radiation heat transfer through the surfaces except the top surface (S_0) for spectral measurement. However, only one face (S_1) of the sample was coated with colloidal graphite (Acheson, Electrodag 188) over the metal coating so as to absorb the radiation from the heater. It is important to note that the sample is actually heated by conduction, since the composite surface of a metal and an absorber works as a conductive heater attached to the sample without spacing. These sample treatments seem to be good for the one-dimensional heat flow in the sample.

The normal emission spectrum from the clear top surface has been measured in the temperature range from 400 K to 850 K at steady state. The temperature inside the sample was monitored at two points using sheathed thermocouples

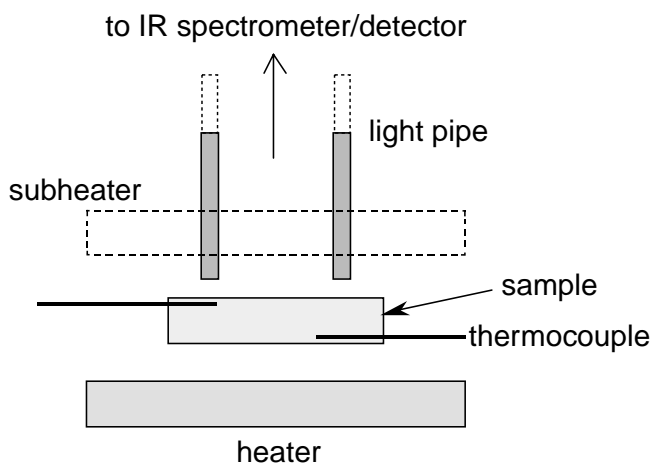


Fig. 1. Schematic configuration of TRAC for spectral measurement. The dimensions of the heater and the light pipe are, respectively, 5 × 5 cm² and 20 mm diameter. A sub-heater is used only for a specific heat capacity measurement.

mounted near the surfaces, as illustrated in Fig. 1. The diameter of the sheath was 0.5 mm and the distance between the two planes, parallel to the disk surface, including each thermocouple was 3.86 ± 0.05 mm. The dimensions of the thermocouple holes were 0.75 mm in diameter and 7 mm in depth. Slight clearances between the sheath and the sample were filled with a graphite adhesive to achieve good thermal contact between them. The surface temperatures are obtained assuming a linear temperature distribution within the sample. A Jasco 610 FTIR spectrometer with a CsI beam splitter and a DLTGS detector is employed for the spectrum measurement at 16 cm⁻¹ resolution.

3.2 Heat capacity measurement by quasi-static TRAC

For the heat capacity measurement, one more heater was mounted over the sample, as indicated by the broken line in Fig. 1. This configuration is essentially the same as that described elsewhere.⁴⁾ A disk-shaped sample of 3 mm thickness and 24 mm diameter was used for the heat capacity measurement. A copper disk, which is 99.9% pure, with the same dimensions as the sample is used as a reference material to evaluate E_h . All the surfaces of the sample were coated with copper by vacuum evaporation before blackening in order to shield the radiation from inside the sample. The blackening material for the heat capacity measurement was a mixture of colloidal graphite and MnO₂ powder (1 : 1, wt%). The hemispherical total emissivity of the present blackening material has been estimated to be 0.93 ± 0.03 below 1000 K.⁴⁾ Instead of the heater temperature, the radiant power $W_h = I_h G$ from the heater was measured directly using a pyroelectric infrared detector, where G is a gain factor of the detector. The calibration factor E_h/G for the present configuration was about 1.26 ± 0.03 (arb. units) throughout the entire temperature range investigated. The rate of the sample temperature was controlled to be about 5 K/min for both heating and cooling modes.

4. Results and Discussion

4.1 IR spectra and hemispherical total emissivity

Open circles in Fig. 2 indicate the normal emission spectrum $\varepsilon(\nu, 0)$ of 5.3 wt% yttria-stabilized tetragonal zirconia measured at surface temperature $T_0 = 523$ K. The closed circles show the hemispherical emission spectrum ε_ν calculated

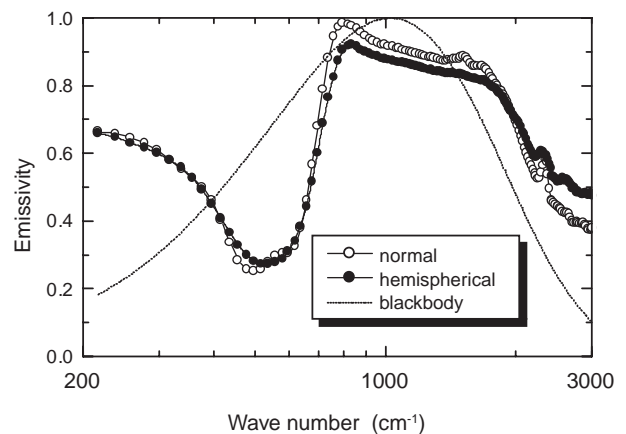


Fig. 2. Emission spectra of 5.3 wt% yttria-stabilized tetragonal zirconia measured at $T_0 = 523$ K. Wave number dependence of blackbody radiation intensity $e_b(\nu)$ is also illustrated by a dotted line.

from eq. (2). The dotted line indicates the normalized spectrum of the blackbody radiation $e_b(\nu) = W(\nu, T)/W(\nu_p, T)$, where ν_p is the peak frequency of $W(\nu, T)$. In order to determine unknown parameters of n_∞ , ν_L and ν_T in eq. (11), we measured reflection spectra of 5.3 wt% yttria stabilized tetragonal zirconia at room temperature using a different spectrometer. Figure 3 plots the room-temperature “emissivity” $(1 - R)$ translated from the reflection spectrum R of the metal-backed sample of 5 mm thickness. From a preliminary analysis of the reflection spectra, $n_\infty = 2.25$, $\nu_L = 690 \text{ cm}^{-1}$ and $\nu_T = 380 \text{ cm}^{-1}$ were obtained. In Fig. 2, ν_R is read as about 820 cm^{-1} , which is in good agreement with that in Fig. 3. The real and imaginary parts of the refractive index obtained from the Kramers-Krönig analysis are shown in Fig. 4. We have also measured the reflection spectrum of 5.3 wt% yttria-stabilized tetragonal zirconia with 5 mm thickness in free space. However, we could not find any difference between the metal-backed sample and the free sample. This implies that a radiation heat flow inside the sample, which possibly occurs above ν_R , is apparently absorbed within the sample and does not come out from the sample. If the apparent absorption in the sample was not so large, the spectrum $(1 - R)$ might show a response similar to the emission spectrum above ν_R because of the reflection by the metal deposited on the back surface.

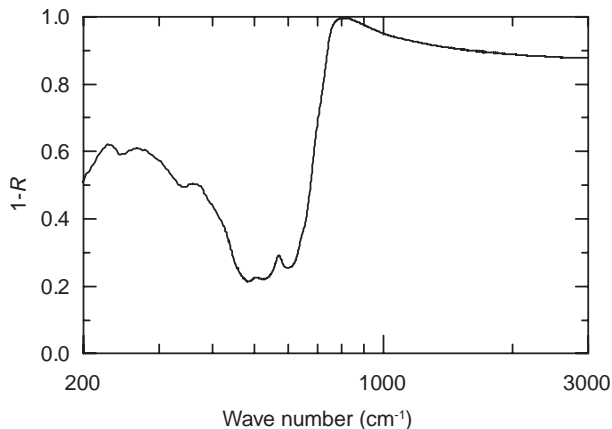


Fig. 3. Room temperature “emissivity” $(1 - R)$ of 5.3 wt% yttria-stabilized tetragonal zirconia obtained from the normal reflection spectrum R .

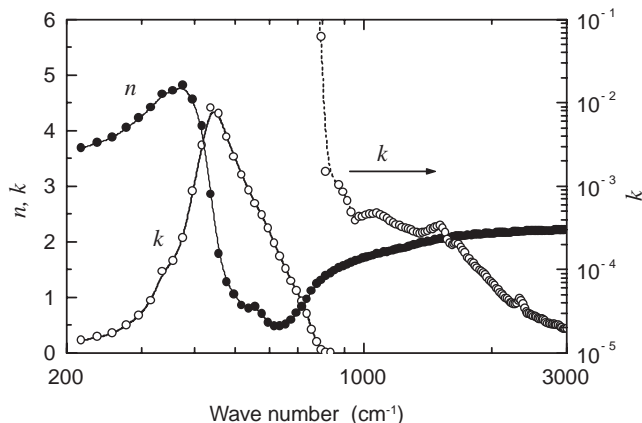


Fig. 4. Refractive index of 5.3 wt% yttria-stabilized tetragonal zirconia at $T_0 = 523 \text{ K}$. Solid circle indicates the real part n , and the open circle the imaginary part k .

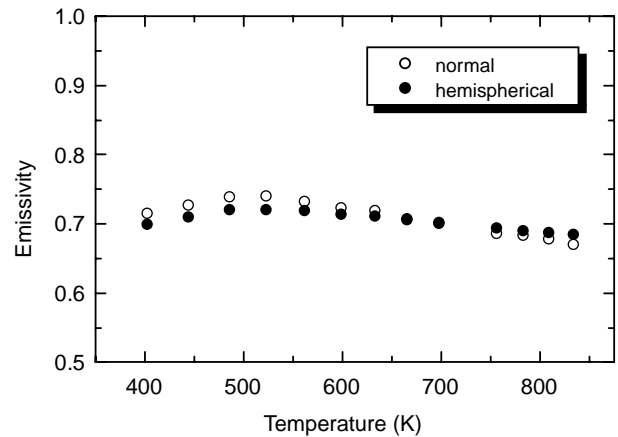


Fig. 5. Total emissivity of 5.3 wt% yttria-stabilized tetragonal zirconia.

Figure 5 shows the normal and hemispherical total emissivities calculated from eq. (3) at various temperatures. In the Kramers-Krönig analysis, we assumed that the values of n_∞ , ν_L and ν_T are independent of temperature. It should be noted that these values were not sensitive to the hemispherical emissivity plotted in Fig. 5. Even if we changed ν_T , for example, as 10% in eq. (11) for eq. (10), the resulting deviation in the emissivity was less than 1%. On the other hand, n_∞ and ν_L are sensitive to the connectivity between eqs. (8) and (10) around ν_R . Therefore, the actual margins allowed for these values were not large, about 2.5% for ν_L and 0.5% for n_∞ .

Olson and Morris¹⁶⁾ reported *normal* total emissivities ranging from 0.5 to 0.9 at high temperature for different zirconia samples. They were obtained by a nonspectroscopic (direct) measurement of thermal radiation from samples in air. While the emissivity strongly depends on the thickness of the sample, it is not shown in their report on zirconia. Furthermore, the materials doped for stabilization are quite different from that in the present sample. Therefore, we cannot directly compare the present result with the previous ones.¹⁶⁾ The important point to note is that the emissivity plotted in Fig. 5 corresponds to that of the sample with thickness 10 mm in free space, since the present sample is metal-backed. We believe that the present method provides basic and important information for further applications, since the total hemispherical emissivity can be obtained spectroscopically without referring to other thermophysical properties of the sample material.

4.2 Thermal conductivity

Figure 6 shows the temperature difference $T_1 - T_0$ between the two surfaces S_1 and S_0 of the sample. Although the value of $T_1 - T_0$ increases with temperature, the ratio of $(T_1 - T_0)/T_0$ is about 0.04 at 834 K. This seems to support a linear approximation for a temperature distribution in the sample. The temperature of the chamber T_r was kept at 290.6 K during the measurements. Now we can evaluate the thermal conductivity from the data of Figs. 5 and 6 with eq. (1). Figure 7 shows the thermal conductivity of the tetragonal zirconia stabilized by 5.3 wt% yttria. The solid symbols indicate the present results. The solid curve is illustrated after an interpolation of data by Slifka *et al.*¹¹⁾ They obtained data using a one-side-guarded hot plate method. The concentration of yttria in the present sample is almost the same as that used in ref. 11. As

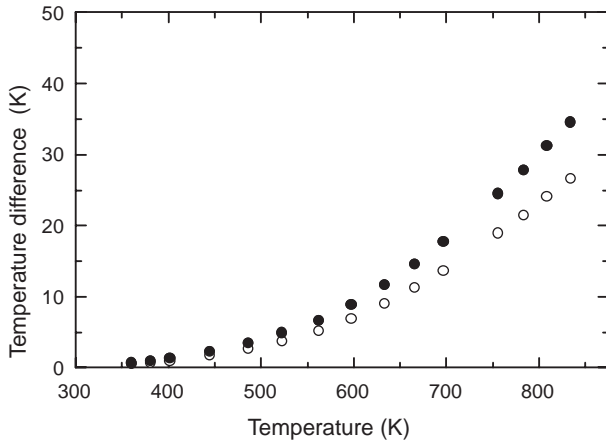


Fig. 6. Temperature difference between surfaces (●) and between thermocouples (○) for the sample with 5 mm thickness. The thermocouple hole separation normal to the disk surface is 3.86 ± 0.05 mm.

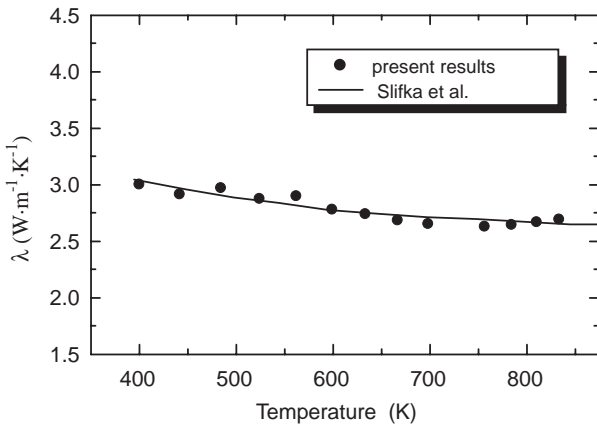


Fig. 7. Thermal conductivity of 5.3 wt% yttria-stabilized tetragonal zirconia.

is easily seen, the present results by spectral TRAC are comparable with those by the other method. From the viewpoint of eq. (1), we believe that the present procedure for deriving the hemispherical total emissivity from the normal emission spectrum is reliable.

4.3 Effects of radiation heat transfer

Let us consider the effect of radiation heat transfer in the sample. This might become an error source in the values of thermal conductivity through ϵ . If the radiation scattering in a medium can be neglected, the effect is estimated by analogy with a case of gray gas.¹⁷⁾ Since we can consider $T_1 - T_0 \ll T_0$ and a linear temperature gradient in the slab mentioned above, we can write the emissivity as

$$\epsilon \approx \epsilon_1 + \epsilon_2(1 + \delta), \quad (15)$$

where ϵ_1 and ϵ_2 are, respectively, the emissivities below and above ν_R . The effect of excess heat flow by radiation is characterized by a factor δ in eq. (15). These quantities can be calculated as follows:

$$\epsilon_1 = \frac{\int_0^{\nu_R} \epsilon_\nu W(\nu, T) d\nu}{\int_0^\infty W(\nu, T) d\nu}, \quad (16)$$

$$\epsilon_2(1 + \delta) = \frac{\int_{\nu_R}^\infty \epsilon_\nu W(\nu, T) d\nu}{\int_0^\infty W(\nu, T) d\nu}, \quad (17)$$

$$\delta = \frac{4}{\alpha_p d} \left(\frac{T_1 - T_0}{T_0} \right) \tanh \left(\frac{-\alpha_p d}{2} \right), \quad (18)$$

where α_p is Planck's mean absorption coefficient above ν_R given by

$$\alpha_p = \frac{\int_{\nu_R}^\infty \alpha(\nu) W(\nu, T) d\nu}{\int_0^\infty W(\nu, T) d\nu}, \quad (19)$$

with $\alpha(\nu) = 4\pi\nu k(\nu)$. For a sample with a large absorbance coefficient above ν_R , eq. (15) becomes $\epsilon \approx \epsilon_1 + \epsilon_2$ since $\delta \approx 0$ for $\alpha_p d \gg 1$. If transmission occurs at a frequency higher than the peak of blackbody radiation at the sample temperature, the contribution of $\epsilon_2\delta$ to the total emissivity may not be large. From these points of view, the spectral TRAC method can be applied for materials with high LO mode frequency (or ν_R) and large absorption ($\alpha_p d$) above ν_R . At high temperature, however, the contribution of $\epsilon_2\delta$ will increase and be followed by Wien's displacement law for blackbodies. In the case of small absorption also, some errors will be contained in ϵ . The ratio of excess emissivity to total emissivity, $\epsilon_2\delta/(\epsilon_1 + \epsilon_2)$, calculated from the measured emission spectra, is shown in Fig. 8. Although it increases with temperature, it still remains at less than 5.3% at high temperature. However, actual contribution of the radiation heat transfer seems to be considerably small, since there are no differences between the metal-backed and free samples in reflectivity. In other words, the radiation is almost completely absorbed in the sample. It should be noted that the density of the present sample is 2.5% higher than that previously reported for 5.3% yttria-stabilized zirconia.^{11,13)} This absorption mechanism may be attributed to the radiation scattering by grain boundaries of the ceramic sample. This process may also decrease the temperature deviation from a linear distribution caused by the radiation in the sample. Anderson *et al.*¹⁹⁾ reported that the deviation in a fused quartz plate of thickness 12.7 mm, given 200 K difference in the surface temperatures around 930 K, was about 5 K. In the present case, the temperature difference is about 30 K

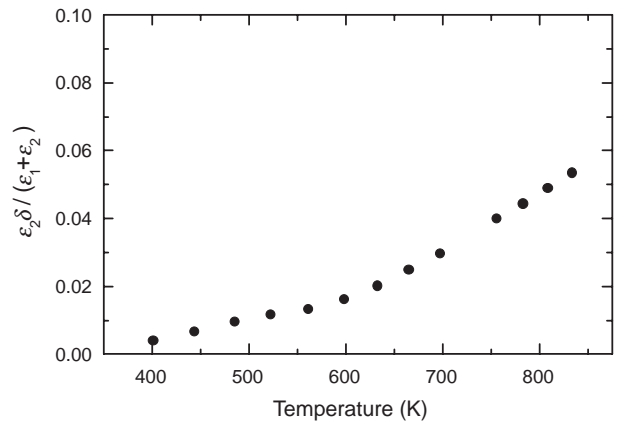


Fig. 8. Ratio of excess emissivity above the LO mode frequency to total emissivity.

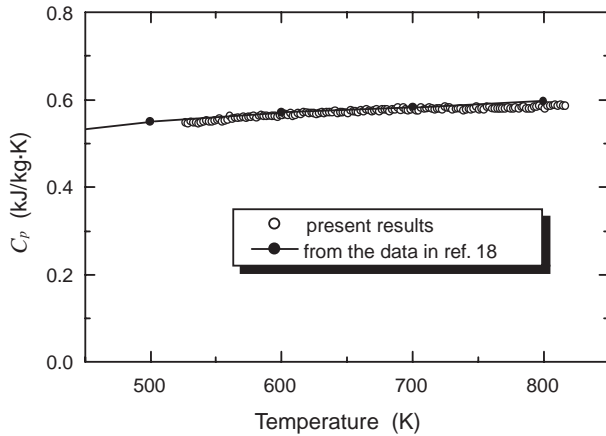


Fig. 9. Specific heat capacity of zirconia.

at 800 K for the 5-mm-thick disk. Therefore, we consider that the deviation in the present samples is presumably less than about 0.5 K at high temperature and the resulting error in their thermal conductivity is less than 1%.

4.4 Specific heat capacity

Figure 9 shows the specific heat capacity of zirconia ceramics. Open circles are plotted after averaging the values obtained by several scans of TRAC for a tetragonal zirconia stabilized by 5.3 wt% yttria. Data of monoclinic ZrO_2 reported in the literature¹⁸⁾ are also indicated by solid circles. The solid line is illustrated after an interpolation using the data in ref. 18. As is evident in Fig. 9, the present results are very close to those of the monoclinic sample. This is consistent with the results of Hasselmann *et al.*¹³⁾ that specific heat is almost independent of the yttria concentration as a stabilizer.

5. Conclusions

The hemispherical total emissivity of a ceramic sample of 5.3 wt% yttria-stabilized (tetragonal) zirconia has been obtained from a spectral analysis of the normal emission spectrum based on Kramers-Krönig relations and virtual mode equations. What is significant in this method is that the hemispherical total emissivity is derived independently of other thermophysical quantities, that is, specific heat, thermal diffusivity and thermal conductivity. With this emissivity, we

have obtained the values of thermal conductivity at steady state. The present results are comparable with those obtained by other techniques,¹¹⁾ confirming the validity of the method examined here. The error caused by the radiation heat transfer due to transmission in the high-frequency region has been estimated as a function of temperature. If the radiation scattering in the sample were neglected, the error might increase gradually with temperature (up to 5.3% at 850 K). It is suggested, however, that the radiation scattering in the ceramic sample may compensate for the effects of the radiation heat transfer on the value of thermal conductivity. In addition, the specific heat capacity has been obtained by quasi-static TRAC. The values are very close to those of a monoclinic phase.

- 1) K. Hisano and T. Yamamoto: *High Temp. & High Press.* **25** (1993) 337.
- 2) K. Hisano: *Int. J. Thermophys.* **18** (1997) 535.
- 3) K. Hisano, S. Sawai and K. Morimoto: *Int. J. Thermophys.* **20** (1999) 733.
- 4) K. Morimoto, S. Sawai and K. Hisano: *Int. J. Thermophys.* **20** (1999) 709.
- 5) H. Tanaka, S. Sawai, K. Morimoto and K. Hisano: *Int. J. Thermophys.* **21** (2000) 927.
- 6) R. Fuchs, K. L. Kliewer and W. J. Pardee: *Phys. Rev.* **150** (1966) 589.
- 7) G. Teufer: *Acta Crystallogr.* **15** (1962) 1187.
- 8) D. K. Smith and C. F. Cline: *J. Am. Ceram. Soc.* **45** (1962) 249.
- 9) C. Pascual and P. Duran: *J. Am. Ceram. Soc.* **66** (1983) 23.
- 10) I. D. McCullough and K. N. Trueblood: *Acta Crystallogr.* **12** (1959) 507.
- 11) A. J. Slifka, B. J. Filla and J. K. Stalick: *Thermal Conductivity 25, Proc. 25th Int. Thermal Conductivity Conf. and 13th Int. Thermal Expansion Conf. Ann Arbor, Michigan, 1999*, eds. C. Uher and D. Morelli (Technomic, Lancaster, 2000) p. 147.
- 12) K. An, K. S. Ravichandran, R. E. Dutton and S. L. Semiatin: *J. Am. Ceram. Soc.* **82** (1999) 399.
- 13) D. P. H. Hasselmann, L. F. Johnson, L. D. Bentsen, R. Syed, H. L. Lee and M. V. Swain: *Am. Ceram. Soc. Bull.* **66** (1987) 799.
- 14) T. O. McMahon: *J. Opt. Soc. Am.* **40** (1950) 276.
- 15) K. Hisano: *J. Phys. Soc. Jpn.* **25** (1968) 1091.
- 16) O. H. Olson and J. C. Morris: *WADC Tech. Rep.* **56-222** (1960) Pt. III, p. 1.
- 17) R. Siegel and J. R. Howell: *Thermal Radiation Heat Transfer* (Taylor & Francis, Washington D.C., 1992).
- 18) P. Gordon and A. R. Kaufmann: *USAFEC Publ. AECD-2683* (1950) 1; through *Thermophysical Properties of High Temperature Solid Materials*, ed. Y. S. Touloukian (Macmillan, New York, 1967) Vol. 4, Pt. I, p. 576.
- 19) E. E. Anderson, R. Viskanta and W. H. Stevenson: *J. Heat Transfer* **95** (1973) 179.